

***Supporting Information for Chem Comm article:***

**“Near-infrared light-triggered irreversible aggregation of  
poly(oligo(ethylene glycol) methacrylate)-stabilised  
polypyrrole nanoparticles under biologically relevant  
conditions”**

Kin Man Au,<sup>§*a*</sup> Mei Chen,<sup>§*b*</sup> Steven P. Armes\*<sup>*a*</sup> and Nanfeng Zheng\*<sup>*b*</sup>

<sup>*a*</sup> Department of Chemistry, The University of Sheffield, Brook Hill, Sheffield, South Yorkshire, S3 7HF, UK.

Email: s.p.armes@shef.ac.uk (S.P.A.)

Tel: +44 (0) 114 222 29342

<sup>*b*</sup> State Key Laboratory for Physical Chemistry of Solid Surfaces and Department of Chemistry, College of Chemistry and Chemical Engineering, Xiamen University, Xiamen 361005, China.

Email: nfzheng@xmu.edu.cn (N.F.Z.)

Tel: +86 592 2186821

<sup>§</sup> K.M.A. and M.C. contributed equally to this work.

\* Corresponding authors.

## Section S1: Experimental details

### S1.1. Materials

Pyrrrole (> 98 %) was purchased from Aldrich. It was purified by passing through a column of activated basic alumina and stored in the dark at - 20 °C before use. Iron(III) trichloride hexahydrate ( $\text{FeCl}_3 \cdot 6\text{H}_2\text{O}$ , ACS reagent, 98.0-102.0 %), sodium tosylate (NaOTs, 95 %), and fatty acid- and globulin-free bovine serum albumin (BSA, BioXtra,  $\geq 98$  %) were purchased from Aldrich and used without further purification. The synthesis and characterisation of poly(2-(methacryloyloxy)ethylaminocarboxymethyl)thiophene – *stat* – oligo(ethylene glycol) methacrylate) (hereafter denoted as poly(2TMOI-OEGMA)) was reported in supporting reference 1. Each OEGMA repeat unit contains an average of 7 ethylene glycol (-CH<sub>2</sub>CH<sub>2</sub>O-) repeat units and the copolymer contains 10 mol % 2TMOI repeat unit, as previously determined by <sup>1</sup>H NMR spectroscopy.<sup>1</sup> The number-average molecular weight ( $M_n$ ) of the copolymer was found to be 31,200 g mol<sup>-1</sup> (polydispersity =  $M_w/M_n = 1.59$ ) vs poly(methyl methacrylate) standards, as previously determined by THF GPC.<sup>1</sup> Phosphate buffered saline (PBS) tablets were purchased from Oxoid Ltd. (U.K.). Each 0.10 M PBS solution contained 137 mM sodium chloride (NaCl), 2.7 mM potassium chloride (KCl), 10 mM disodium phosphate ( $\text{Na}_2\text{HPO}_4$ ), and 1.76 mM potassium dihydrogen phosphate ( $\text{KH}_2\text{PO}_4$ ). The 0.10 M PBS was adjusted to pH 7.0 using 0.50 M HCl before use.

### S1.2. Characterisation

#### S1.2.1. Dynamic light scattering (DLS) and aqueous electrophoresis

Dynamic light scattering studies were conducted at 25 °C using a Malvern Zetasizer Nano ZS instrument equipped with a 4 mW He-Ne solid-state laser operating at 633 nm. Backscattered light was detected at 173°, and the intensity-average diameter ( $D_h$ ) was calculated over fifteen runs of 15 seconds duration from the quadratic fitting of the correlation function using the Stokes-Einstein equation. The viscosity and complex refractive index of H<sub>2</sub>O, 0.10 M PBS and isopropanol were provided by Malvern Ltd. (UK). The polydispersity index (PDI) was calculated from the cumulants analysis of the correlation function. All measurements were performed in triplicate.

*In situ* variable temperature DLS measurements were conducted using the same Malvern Zetasizer Nano ZS instrument, except 10 mm path length glass cuvettes were used instead of disposable polystyrene cuvettes. The step size of each *in situ* measurement is 2.5 °C

from 20 to 90 °C. Samples were heated at a heating rate of 2.0 °C min<sup>-1</sup> and an equilibrium time of 3 minutes. Each measurement was averaged over ten 12 second scans.

*Time dependent DLS* measurements were conducted using the same Malvern Zetasizer Nano ZS instrument. As for the *in situ* variable temperature measurements, 10 mm path length glass cuvettes were used in the studies. Prior to each time dependent measurement, the DLS instrument and an empty glass cuvette were pre-equilibrated at a desired temperature (50 – 75 °C) for 2 minutes. For each measurement, 1.5 mL of PPy nanoparticle dispersion was transferred to the pre-heated instrument and equilibrated for 3 min. before the first measurement (ten 12 second scans). Further measurements were repeated every 3 minutes for up to 33 minutes.

Aqueous electrophoresis measurements were also conducted using the same Malvern Zetasizer Nano ZS instrument using slow field reversal (SFR) and fast field reversal (FFR) phase analysis light scattering (M3-PALS) technique using either 1.0 mM KCl or 0.10 M PBS as background electrolyte. Zeta potentials were calculated from electrophoretic mobilities using the Smoluchowski relationship. The solution pH was adjusted manually by the addition of either 0.10 M HCl or 0.10 – 0.01 M NaOH solution. All measurements were performed in triplicate. All light scattering data were processed using Malvern Zetasizer Software version 6.20. The viscosities and dielectric constants of 0.10 M PBS were provided by Malvern Ltd. (UK).

### **S1.2.2. Disc centrifuge photosedimentometry (DCP)**

DCP analyses were conducted using a CPS Instruments Ltd. Disc Centrifuge Model 24000. Particle densities were determined by helium pycnometry prior to DCP analysis. A density gradient was constructed from 8% to 24 % sucrose solutions for the PPy nanoparticles. A 263 nm diameter poly(vinyl chloride) latex was used for calibration (CPS Instruments Ltd.) prior to the analysis of each sample when using the 8 % to 24 % sucrose gradient. Typical running times were between 10 and 15 minutes at a centrifugation rate of 20,000 rpm. The sucrose gradient was changed after the characterisation of each BSA-nanoparticle mixture to prevent excess BSA from interfering with further analyses as previously reported.<sup>1</sup> The data were processed using the CPS Disc Centrifuge Control System (version 9.5, CPS Instruments Ltd.). The colloidal stability and antifouling properties of POEGMA-stabilised PPy nanoparticles were assessed by DCP according to literature protocol.<sup>1</sup>

### **S1.2.3. Transmission electron microscopy (TEM)**

Samples were prepared by drying a drop (10  $\mu$ L) of highly diluted polypyrrole dispersion onto a carbon-coated grid (Agar Scientific, UK), which was air-dried overnight before analysis using a Philips CM100 or TECNAI F-30 field-emission TEM instrument operating at 100 – 300 kV.

### **S1.2.4. Elemental microanalysis**

POEGMA-stabilised PPy nanoparticles were freeze-dried before elemental microanalysis. Elemental microanalyses were carried out at the Centre for Chemical Instrumentation and Analytical Services in the Department of Chemistry at The University of Sheffield (UK). Carbon, hydrogen and nitrogen contents were determined by a Perkin Elmer 2400 Elemental Analyser. Chlorine and sulfur contents were determined using the Schoninger flask combustion technique. The C, H, N, Cl and S contents of poly(2TMOI-OEGMA) and PPy bulk powder prepared in the absence of steric stabiliser were previously reported in supporting reference 1.

### **S1.2.5. *In vitro* cell viability assay**

The cytotoxicity of POEGMA-stabilised PPy nanoparticles towards a HeLa cell line was quantified using a 3-(4,5-dimethylthiazolyl-2)-2,5-diphenyltetrazolium bromide (MTT) metabolic assay. Briefly, HeLa cells were harvested at a concentration of  $10^4$  cells/200  $\mu$ L in a 96-wall plate with 0.10 M PBS or 10 – 500  $\mu$ g/mL of POEGMA-stabilised PPy nanoparticles dispersed in 0.10 M PBS at 37 °C under 5 % CO<sub>2</sub> for 48 h. The HeLa cells were then washed with 0.10 M PBS before incubation with 10  $\mu$ L of 3-(4,5-dimethylthiazolyl-2)-2,5-diphenyltetrazolium bromide (MTT) for an additional 4 h. Dimethyl sulfoxide was then added to the MTT-incubated HeLa cells. The cell viabilities were assessed spectroscopically at an absorbance wavelength of 575 nm using a reference wavelength of 650 nm.

### **S1.2.6. UV-visible-NIR spectroscopy**

UV-visible-NIR absorption spectra of POEGMA-stabilised PPy nanoparticles dispersed in H<sub>2</sub>O were recorded using a Perkin Elmer Lambda 900 UV-visible-NIR spectrometer at 20 °C. The solids content of the purified POEGMA-stabilised PPy nanoparticles was first determined by a moisture analyser (Ohaus MB45 Moisture Analyser Balance) before being diluted to desired concentrations for further studies (include UV-

visible-NIR spectroscopic studies). All measurements were performed using disposable 10 mm path-length micro-cuvettes (Brand<sup>TM</sup>).

Variable temperature turbidimetry measurements were performed in a JASCO J-810 Circular Dichroism Spectropolarimeter equipped with a Peltier temperature controller operated in its spectroscopic measurement mode using a 2 mm path length quartz cuvette. The turbidity of the “free” poly(2TMOI-OEGMA) dispersed in H<sub>2</sub>O and 0.10 M PBS (5 mg/mL) was assessed by determining the temperature-dependent extinction at 500 nm. The samples were heated from 20 to 95 °C at a step size of 1.0 °C and a heating rate of 1.0 °C/min (equilibrium time per step = 2 min.).

### **S1.2.7. Differential scanning calorimetry (DSC)**

The thermal profiles of the “free” poly(2TMOI-OEGMA) and POEGMA-stabilised PPy nanoparticles dissolved/dispersed in H<sub>2</sub>O and 0.10 M PBS were recorded using a VP-DSC MicroCalorimeter (MicroCal LCC, USA) operating at a heating rate of 1.0 °C min<sup>-1</sup>, a step size of 1.0 °C and an equilibrium time of 2 minutes per step from 20 to 95 °C. Buffer-buffer or water-water baselines were subtracted from the sample data.

### **S1.2.8. Photothermal heating experiments**

Photothermal heating experiments were performed using an optical fibre-coupled NIR laser diode (2W; BWT Beijing Co., Ltd., China) operating at a wavelength of 808 nm (power density = 1.0 W cm<sup>-2</sup>). The temperatures of all PPy nanoparticle dispersions were monitored by infrared thermography (HM-300; Guangzhou SAT Infrared Technology Co., Ltd, China) during NIR irradiation experiments.

## **S1.3. Synthesis**

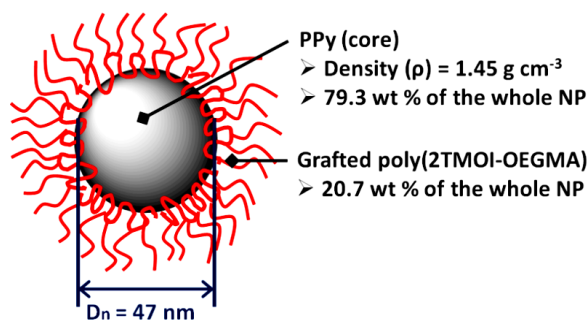
### **S1.3.1. Synthesis of POEGMA-stabilised PPy nanoparticles**

Tosylate-doped POEGMA-stabilised PPy nanoparticles of about 50 nm diameter were synthesised by aqueous dispersion polymerisation, as previously reported.<sup>1</sup> In this study, a higher concentration of poly(2TMOI-OEGMA) (1.5 w/v % instead of 1.0 w/v % used in the previous study<sup>1</sup>) was used in the synthesis of the PPy nanoparticles in order to reduce the size of the nanoparticles. Poly(2TMOI-OEGMA) (1.5 g) was dissolved in deionised water (60 mL) in a 125 mL sealed bottle by stirring (400 rpm) at room temperature for 2 h. Iron(III)

chloride hexahydrate (9.10 g, 33.67 mmol) and sodium tosylate (8.40 g, 43.27 mmol) was dissolved in water (40 mL) in a second sealed bottle. Pyrrole (1.00 mL, 14.41 mmol) and the iron(III) chloride, sodium tosylate mixture were added to the stabiliser solution. Polymerisation was allowed to proceed for 18 h at 20°C. The resulting black dispersion was first filtered through pre-washed glass wool under gravity before being centrifuged at 15,000 rpm for 1 h and the resulting black sediment was redispersed in deionised water by sonication for 1 h. This centrifugation-redispersion cycle was repeated seven times to remove all traces of spent oxidant and non-grafted copolymer stabiliser. The polypyrrole particles were further purified by filtration through pre-washed glass wool to remove any aggregated particles before further characterisation.

## Section S2: Supporting calculations

### Supporting calculation 1: Mean PPy nanoparticle mass and steric stabiliser grafting density



Mean mass of each POEGMA-stabilised PPy nanoparticle (NP)

= Volume of each PPy NP  $\times$  density of bulk PPy  $\div$  weight fraction of PPy ( $F_{PPy}$ )

$$= \frac{4}{3} \pi r^3 \times \rho_{PPy} \div F_{PPy} = \frac{4}{3} \pi (23.5 \text{ nm})^3 \times (1.45 \text{ g cm}^{-3}) \div (0.793) = \underline{9.9 \times 10^{-17} \text{ g}}$$

Hence,  $10 \text{ mg dm}^{-3}$  of POEGMA-stabilised PPy nanoparticles contains 168 picomoles of nanoparticles and  $1000 \text{ mg dm}^{-3}$  of POEGMA-stabilised PPy nanoparticles contains 16.8 nanomoles of nanoparticles.

Assuming all the copolymer stabiliser was grafted onto the surface of the nanoparticle (NP) during dispersion polymerisation, the steric stabiliser surface grafting density ( $\Gamma$ ) is given by:

$$\begin{aligned}\Gamma &= \text{mean mass of poly(2TMOI-OEGMA) in each PPy NP} \div \text{surface area of PPy NP} \\ &= \text{Weight of each PPy NP} \times \text{weight fraction of poly(2TMOI-OEGMA)} \div \text{surface area of PPy NP} \\ &= (9.9 \times 10^{-17} \text{ g}) \times (0.207) \div 4\pi(23.5 \text{ nm})^2 \\ &= \mathbf{3.0 \text{ mg m}^{-2}}\end{aligned}$$

This surface grafting density of the POEGMA-stabilised PPy nanoparticles is comparable with other sterically stabilised PPy nanoparticles prepared via aqueous dispersion polymerisation.<sup>1,2</sup>

### Supporting calculation 2: Photothermal transduction efficiency calculation

The photothermal transduction (conversion) efficiency of the POEGMA-stabilised PPy nanoparticles was calculated *via* Roper's method<sup>3</sup> from the steady-state cooling curve recorded for a 20 mg dm<sup>-3</sup> of POEGMA-stabilised PPy nanoparticles aqueous dispersion (Fig. 1d) after the PPy nanoparticles achieved thermal equilibrium (at 38.7 °C) induced by NIR irradiation (808 nm, 1.0 W cm<sup>-2</sup>). Briefly, the photothermal transduction efficiency ( $\eta$ ) of the PPy nanoparticles is given by the following equation,<sup>3-5</sup>

$$\eta = \frac{hS(T_{max} - T_{surr}) - Q_{bis}}{I(1 - 10^{-A_{808nm}})} \quad (1)$$

where  $h$  is the heat transfer coefficient,  $S$  is the surface area of the container,  $T_{max}$  is the maximum steady-state temperature of the NIR-irradiated PPy nanoparticles recorded just before cooling ( $T_{max} = 38.7$  °C),  $T_{surr}$  is the ambient surrounding temperature ( $T_{surr} = 19.5$  °C),  $Q_{bis}$  is the heat dissipated from light absorbed by the sample vial,  $A_{808nm}$  is the absorbance the NIR absorber (absorbance of 20 mg dm<sup>-3</sup> of PPy nanoparticles at 808 nm = 0.739; Fig. S6a, ESI†).  $Q_{bis}$  was measured by filling a sample vial with 1.0 mL of water (instead of 1.0 mL of PPy nanoparticles).  $Q_{bis}$  was measured to be 9.7 mW. Constants  $h$  and  $S$  cannot be measured accurately during NIR irradiation, but they can be calculated from the thermal time constant for cooling ( $\tau_c$ ), which is equivalent to the rate of heat transfer from the NIR-irradiated sample to its surroundings. Mathematically, the thermal time constant for cooling ( $\tau_c$ ) is related to the constants  $h$  and  $S$  by the following equation,

$$\tau_c = \frac{m_i C_{p,i}}{hS} \quad (2)$$

where  $m_i$  is the mass of water ( $m_i = 1.0$  g) and  $C_{p,i}$  is the heat capacity of the medium ( $C_{p,i}$  of water =  $4.2 \text{ J g}^{-1} \text{ }^\circ\text{C}^{-1}$ ). The thermal time constant for cooling can be calculated indirectly from the driving force temperature ( $\theta$ ) using the following equation,

$$t = -\tau_c \ln \theta \quad (3)$$

where  $t$  is the cooling time. The driving force temperature ( $\theta$ ) is related to the temperature of the cooling sample ( $T$ ) by the following equation,

$$\theta = \frac{T - T_{surr}}{T_{max} - T_{surr}} \quad (4)$$

Thus the gradient obtained from the plot of natural logarithm of the driving force temperature ( $\ln \theta$ ) as a function of cooling time is equivalent to  $-1/\tau_c$ . As shown in Fig. 1d, the gradient of this plot is  $-0.293 \text{ min}^{-1}$ , hence  $\tau_c = -1/\text{gradient} = 205$  s.

Substituting  $m_i = 1$  g,  $C_{p,i}$  of water =  $4.2 \text{ J g}^{-1} \text{ }^\circ\text{C}^{-1}$ , and  $\tau_c = 205$  s into equation (2), we have,

$$hS = \frac{m_i C_{p,i}}{\tau_c} = \frac{(1 \text{ g})(4.2 \text{ J g}^{-1} \text{ }^\circ\text{C}^{-1})}{(205 \text{ s})} = 20.5 \text{ mW }^\circ\text{C}^{-1}$$

Substituting  $hS = 20.5 \text{ mW }^\circ\text{C}^{-1}$ ,  $T_{max} = 38.7$  °C,  $T_{surr} = 19.5$  °C,  $Q_{bis} = 9.7$  mW,  $I = 1.0$  W, and  $A_{808nm} = 0.739$  into equation (1), the photothermal transduction efficiency of the POEGMA-stabilised PPy nanoparticles at 808 nm,  $\eta$ , is given by:

$$\eta = \frac{hS(T_{max} - T_{surr}) - Q_{bis}}{I(1 - 10^{-A_{808nm}})}$$

$$\eta = \frac{(20.5 \text{ mW }^\circ\text{C}^{-1})(39.7 \text{ }^\circ\text{C} - 19.5 \text{ }^\circ\text{C}) - (9.7 \text{ mW})}{(1000 \text{ mW})[1 - 10^{-(0.739)}]}$$

$$\eta = \frac{384 \text{ mW}}{818 \text{ mW}} = 46.9 \% \approx \underline{\underline{47 \%}}$$

The NIR photothermal transduction efficiency of the tosylate-doped POEGMA-stabilised PPy nanoparticles is significantly higher than other well-documented plasmon resonance nanoparticles, such as gold nanorods ( $\eta = 21$  % at 800 nm),<sup>4</sup> gold nanoshells ( $\eta = 13$  % at 800 nm),<sup>4</sup> and copper selenide nanocrystals ( $\eta = 22$  % at 800 nm,  $\eta = 26$  % at 980 nm),<sup>4,5</sup> determined by the same method. This indicates that the tosylate-doped POEGMA-stabilised PPy nanoparticles behave as a highly efficient NIR photothermal transducer.

### Section S3: Supporting Figures

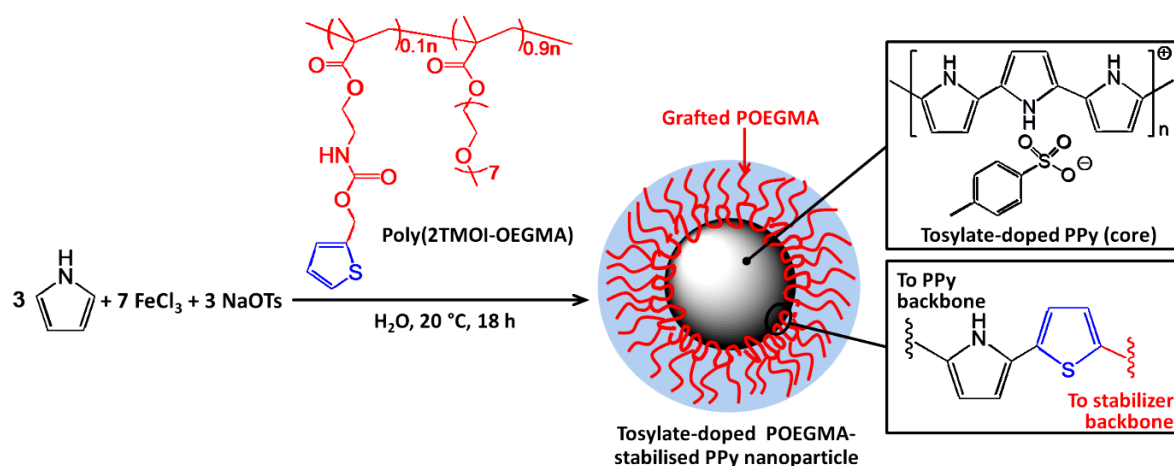


**Fig. S1.** Synthesis of tosylate (OTs<sup>-</sup>)-doped POEGMA-stabilised PPy nanoparticles *via* aqueous dispersion polymerisation of pyrrole using iron(III) trichloride (FeCl<sub>3</sub>) as oxidant and sodium tosylate (NaOTs) as a co-dopant in the presence of 1.5 wt/v % poly(2TMOI-OEGMA) statistical copolymer, which acts as a reactive steric stabiliser. The 2-thiophene ring in the 2TMOI repeat unit ensures chemical grafting of the statistical copolymer onto the PPy nanoparticle surface, as previously reported.<sup>1</sup>

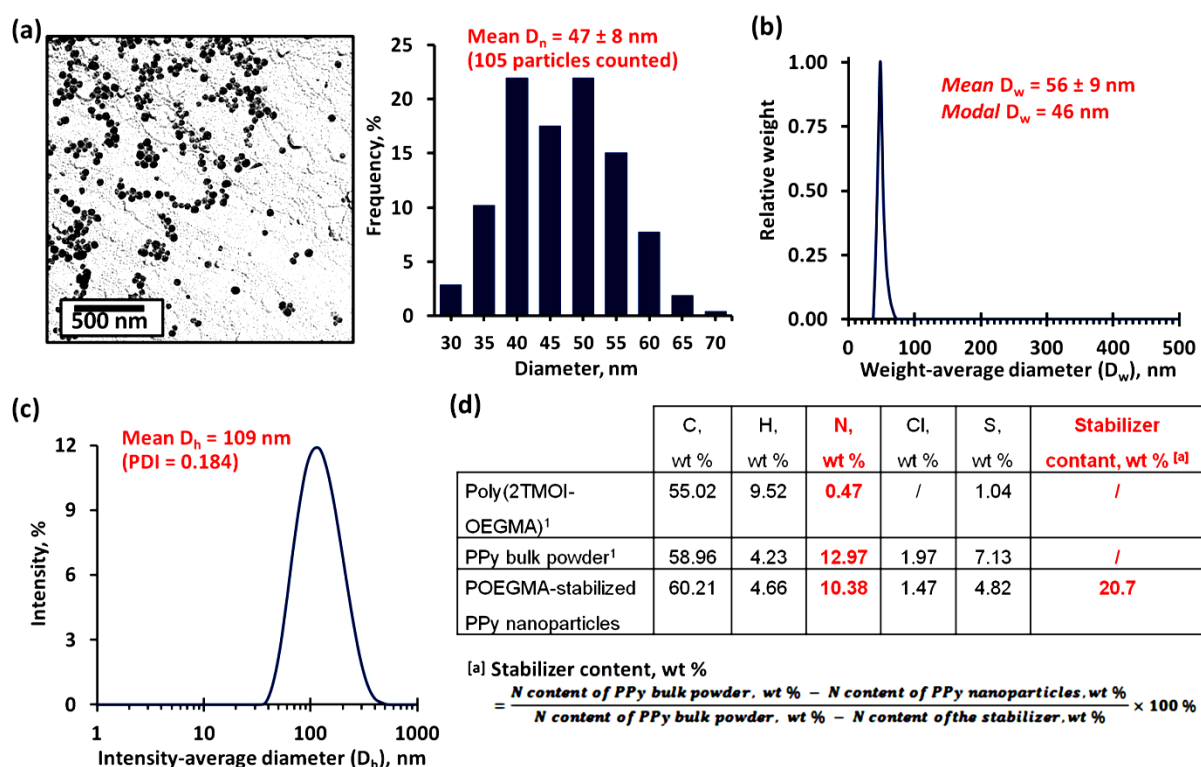


**Fig. S2.** Characterisation of the POEGMA-stabilised PPy nanoparticles. **(a)** Representative TEM image of POEGMA-stabilised PPy nanoparticles. The mean number-average diameter ( $D_n$ ) of the PPy nanoparticles was 47 nm (based on 105 particles counted from the TEM image). **(b)** Weight-average diameter ( $D_w$ ) distribution curve of the POEGMA-stabilised PPy nanoparticles, as measured by DCP. The mean weight-average diameter of the PPy nanoparticles was 56 nm (*modal*  $D_w = 46$  nm) **(c)** Intensity-average diameter distribution curve of the POEGMA-stabilised PPy nanoparticles dispersed in H<sub>2</sub>O at 25 °C, as measured by DLS. The mean intensity-average diameter ( $D_h$ ) of the PPy nanoparticles was 109 nm (PDI = 0.184). By comparing the mean  $D_n$  and mean  $D_h$ , the *upper limit* of the hydrated stabiliser thickness ( $\delta$ ) was calculated to be  $(\delta = 0.5 \times (D_h - D_n))^6 = 32$  nm. **(d)** Table summarising the elemental compositions of poly(2TMOI-OEGMA), PPy bulk powder prepared in the absence of any steric stabiliser and the POEGMA-stabilised PPy nanoparticles used in this study. By comparing nitrogen contents, it was calculated that the POEGMA-stabilised PPy nanoparticles contain 20.7 wt % poly(2TMOI-OEGMA). (N.B. The C, H, N, Cl and S contents of poly(2TMOI-OEGMA) and PPy bulk powder prepared in the absence of steric stabiliser were previously reported in supporting reference 1).

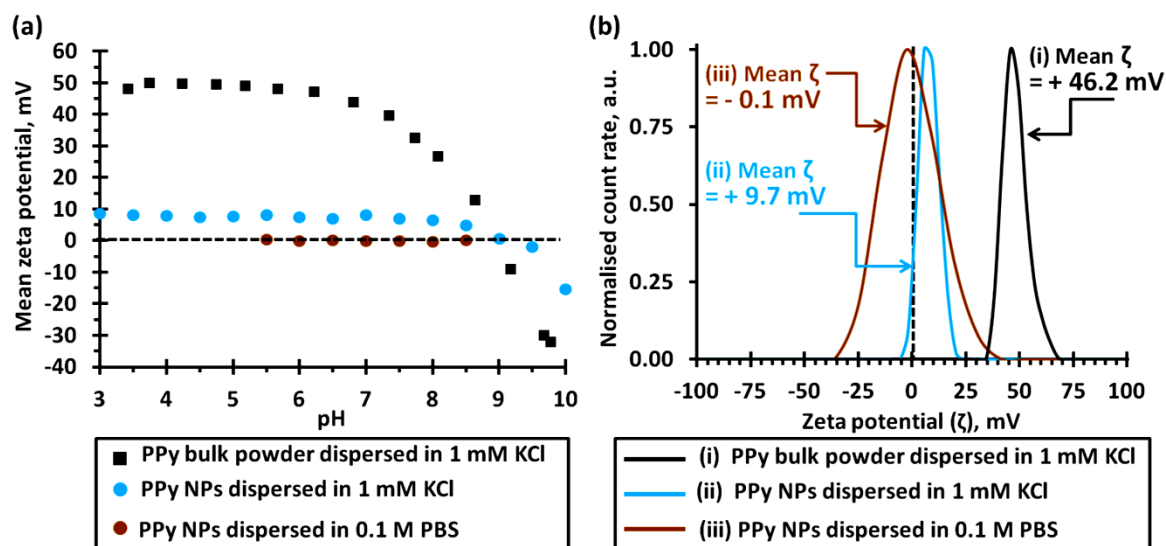


**Fig. S3.** (a) pH-dependent zeta potentials of the tosylate-doped PPy bulk powder dispersed in 1 mM KCl, POEGMA-stabilised PPy nanoparticles (NPs) dispersed in 1.0 mM KCl and 0.10 M PBS. (b) Zeta potential distribution curve of the tosylate-doped PPy bulk powder dispersed in 1.0 mM KCl (at pH 7.0), and POEGMA-stabilised PPy nanoparticles dispersed in 1.0 mM KCl (at pH 7) and 0.10 M PBS (at pH 7). The mean zeta potentials ( $\zeta$ ) of the PPy bulk powder and POEGMA-stabilised PPy NPs dispersed in 1.0 mM KCl at pH 7.0 were +46.2 mV and +9.7 mV, respectively. The PPy nanoparticles exhibit lower mean zeta potentials than the PPy bulk powder prepared in the absence of steric stabiliser because the non-ionic POEGMA-based steric stabiliser on the nanoparticle surface efficiently shields the cationic PPy backbone. The mean zeta potential of the POEGMA-stabilised PPy nanoparticles is reduced to around 0 mV when dispersed in 0.10 M PBS (at pH 5.5 – 7.5) due to compression of electrical double layer in the physiological buffer (ionic strength of PBS  $\approx$  153 mM NaCl). The non-ionic character of the POEGMA-stabilised PPy nanoparticles should prevent non-specific protein-nanoparticle and cell-nanoparticle interactions. (N.B. The zeta potential data for PPy bulk powder were previously reported in supporting reference 1).

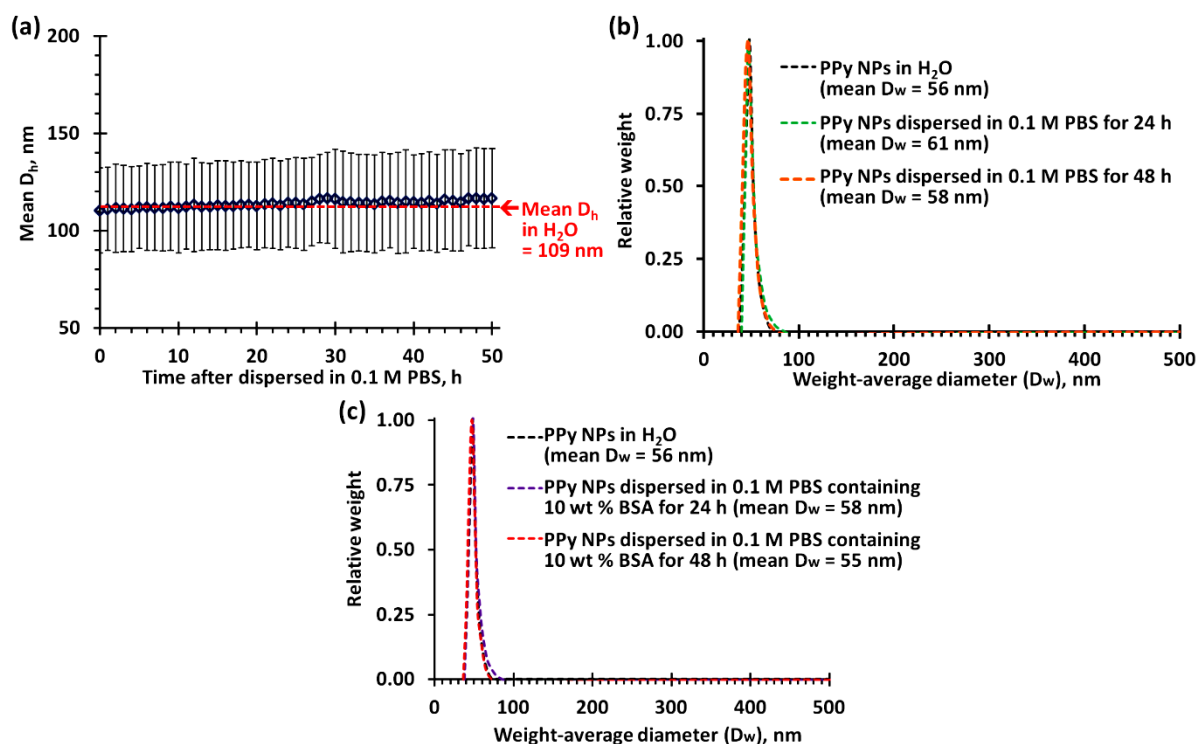


**Fig. S4.** Colloidal stability and anti-biofouling performance of the POEGMA-stabilised PPy nanoparticles under biologically relevant conditions. **(a)** The plot of mean intensity-average diameter ( $D_h$ ) of the POEGMA-stabilised PPy nanoparticles after being dispersed in 0.10 M PBS at 37 °C for up to 48 h. The mean  $D_h$  and polydispersity index (PDI) remained at about 110 nm and 0.190, respectively. **(b)** Weight-average diameter ( $D_w$ ) distribution curves of POEGMA-stabilised PPy nanoparticles recorded before and after being dispersed in 0.10 M PBS at 37 °C for up to 48 h. The mean  $D_w$  of the nanoparticles remained almost constant and the modal  $D_w$  remained at 47 nm, indicating that the PPy nanoparticles remained colloidally stable in the high ionic strength physiological buffer. This is due to the steric stabilisation conferred by the chemically-grafted POEGMA-based steric stabiliser (charge stabilisation can be ruled out as the zeta potential of the PPy nanoparticles is approximately zero in 0.10 M PBS at pH 7; see Fig. S3, ESI†). **(c)** Weight-average diameter ( $D_w$ ) distribution curves of POEGMA-stabilised PPy nanoparticles recorded before and after being dispersed in 0.10 M PBS containing 10 wt % BSA at 37 °C for up to 48 h. The mean  $D_w$  of the nanoparticles remained almost constant and the modal  $D_w$  remained at 47 nm, indicating that these sterically-stabilised PPy nanoparticles have excellent anti-biofouling performance.

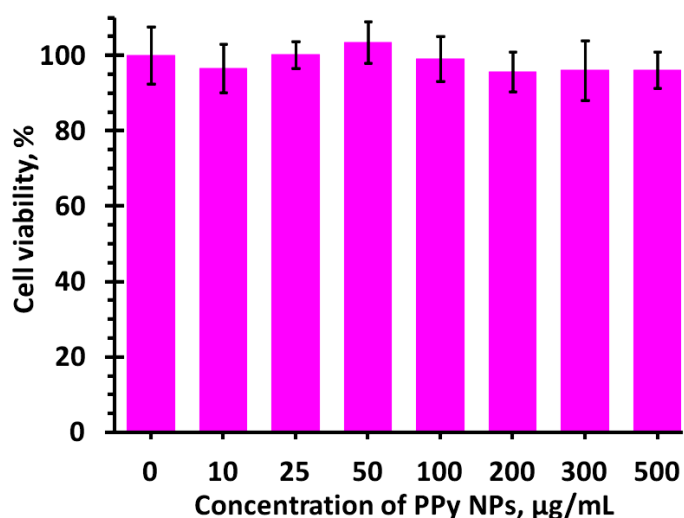


**Fig. S5.** Cytotoxicity of the POEGMA-stabilised PPy nanoparticles under physiological conditions. Cell viability of HeLa cells after incubation with 0 – 500 µg/mL of POEGMA-stabilised PPy nanoparticles dispersed in 0.10 M PBS at 37 °C for 48 h. The cell viability of the HeLa cells were assessed using 3-(4,5-dimethylthiazol-2-yl)-2,5-diphenyltetrazolium bromide (MTT) metabolic assay. The error bars represent standard errors with  $n = 6$ . The cell viability of the HeLa cells is well above 95 % after incubation with 500 mg dm<sup>-3</sup> POEGMA-stabilised PPy nanoparticles dispersed in 0.10 M PBS. The toxicity of the POEGMA-stabilised PPy nanoparticles is significantly lower than similar concentrations of adhesive (biofouling) poly(vinyl alcohol)-stabilised PPy nanoparticles<sup>7</sup> and PPy-coated silica nanoparticles,<sup>8</sup> suggesting that the non-ionic anti-biofouling POEGMA steric stabiliser significantly improves the biocompatibility of PPy nanoparticles. In fact, the toxicity of the POEGMA-stabilised PPy nanoparticles is significantly lower than similar concentrations of PEGylated gold nanorods and gold nanocages.<sup>9</sup>

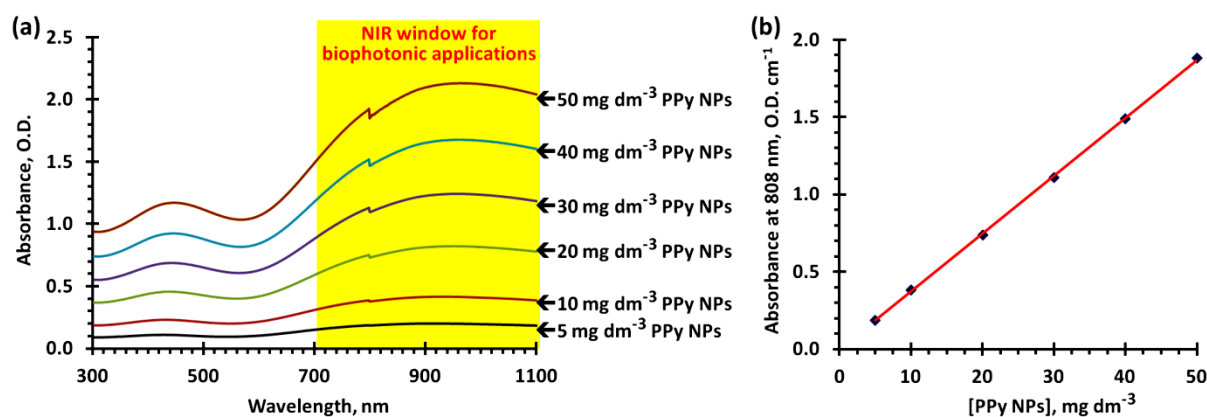


**Fig. S6. (a)** UV-visible-NIR absorption spectra of an aqueous dispersion of 5 – 50 mg dm<sup>-3</sup> POEGMA-stabilised PPY nanoparticles. The absorption band at 446 nm has been assigned to a  $\pi-\pi^*$  electron transition.<sup>10</sup> The broad NIR absorption band at 967 nm has been assigned to bipolaronic electron transfer between the filled valence band and the empty anti-bonding bipolaronic band of doped PPY.<sup>10</sup> The yellow highlighted area shows the NIR “*optical window*” for biophotonic applications, e.g. sub-surface optical imaging, where light scattering by cells and the water absorption spectrum are both relatively weak.<sup>11</sup> **(b)** Plot of absorbance at 808 nm (the emission wavelength of the NIR laser used in the *in vitro* studies) of an aqueous dispersion of 5 – 50 mg dm<sup>-3</sup> POEGMA-stabilised PPY nanoparticles. The absorbance coefficient of the PPY nanoparticles at 808 nm ( $\epsilon_{808}$ ) was calculated to be 37.4 O.D. mg<sup>-1</sup> mL cm<sup>-1</sup>.

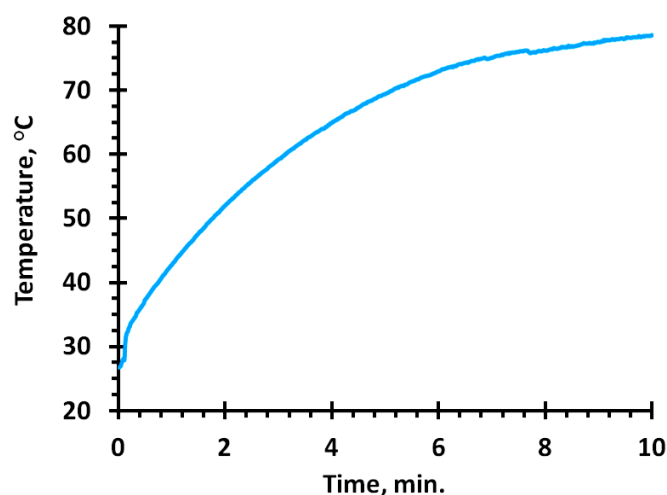


**Fig. S7** Steady-state heating curve recorded for a 500 mg dm<sup>-3</sup> aqueous dispersion of POEGMA-stabilised PPY nanoparticles subjected to NIR irradiation (808 nm, 1.0 W cm<sup>-2</sup>).

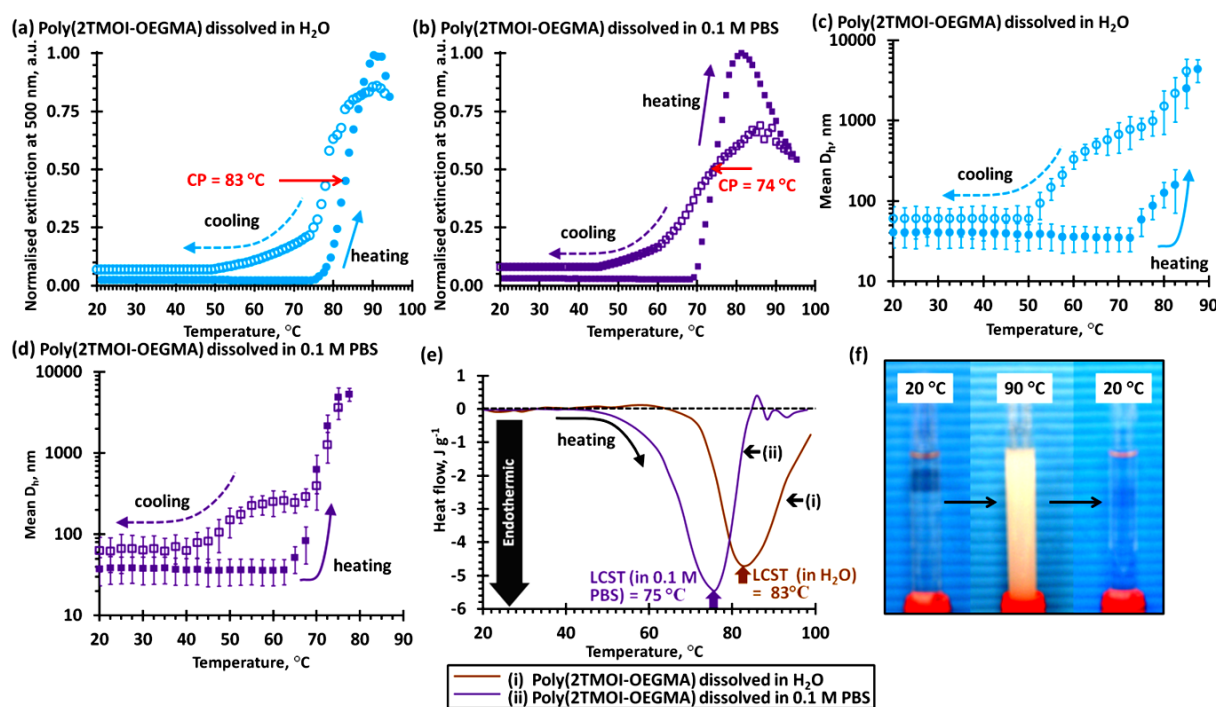


**Fig. S8** Thermo-responsive behaviour of poly(2TMOI-OEGMA) copolymer stabiliser dissolved in either H<sub>2</sub>O or 0.10 M PBS. **(a and b)** Turbidimetry measurements for poly(2TMOI-OEGMA) dissolved in (a) H<sub>2</sub>O and (b) 0.10 M PBS. The cloud point (CP) of poly(2TMOI-OEGMA), which is defined as the maximum change of extinction at 500 nm ( $\Delta\text{Abs}_{500\text{nm}}$ )/change in temperature ( $\Delta\text{Temp}$ ),<sup>12,13</sup> was found to be 83 °C in H<sub>2</sub>O and 74 °C in 0.10 M PBS. This indicates that the LCST-type phase transitions of poly(2TMOI-OEGMA) solutions are at least partially reversible (ca. the normalised extinctions of the poly(2TMOI-OEGMA) solutions at 500 nm only returned to about 0.08 (rather than < 0.01) after cooling from 95 °C to 20 °C). This partial reversible phase transition may be due to cross-linking between the 2TMOI repeat units at elevated temperature. (N.B. These measurements were recorded at a step size of 1 °C, a heating rate of 1 °C/min. and 2 min. equilibrium time prior to each measurement) **(c and d)** *In situ* variable temperature DLS studies of poly(2TMOI-OEGMA) dissolved in (c) H<sub>2</sub>O and (d) 0.10 M PBS. Due to the relatively hydrophobic nature of the 2TMOI repeat units, poly(2TMOI-OEGMA) self-assembles to form micelles in aqueous solution (mean D<sub>h</sub> of the poly(2TMOI-OEGMA) ~ 43 nm and PDI = 0.561 in H<sub>2</sub>O at 20 °C), whereas this copolymer dissolves molecularly in isopropanol (mean D<sub>h</sub> = 10 nm and PDI = 0.246 at 20 °C). The *in situ* variable temperature DLS studies confirm the formation of large micellar aggregates after cooling to 20 °C. **(e)** DSC curves recorded for the poly(2TMOI-OEGMA) dissolved in (i) H<sub>2</sub>O and (ii) 0.10 M PBS. Both poly(2TMOI-OEGMA) aqueous solutions undergo a typical first-order endothermic phase transition.<sup>14</sup> The LCSTs of poly(2TMOI-OEGMA) were found to be 83 °C in H<sub>2</sub>O and 75 °C in 0.10 M PBS, respectively. The LCST values determined by DSC are consistent with the cloud points determined by turbidimetry measurements. (N.B. These measurements were recorded at a step size of 1.0 °C, a heating rate of 1.0 °C min<sup>-1</sup> and 2 min. equilibrium time prior to each measurement) **(f)** Digital photographs of poly(2TMOI-OEGMA) dissolved in 0.10 M PBS recorded at 20 °C, after heating to 90 °C, followed by cooling to 20 °C.

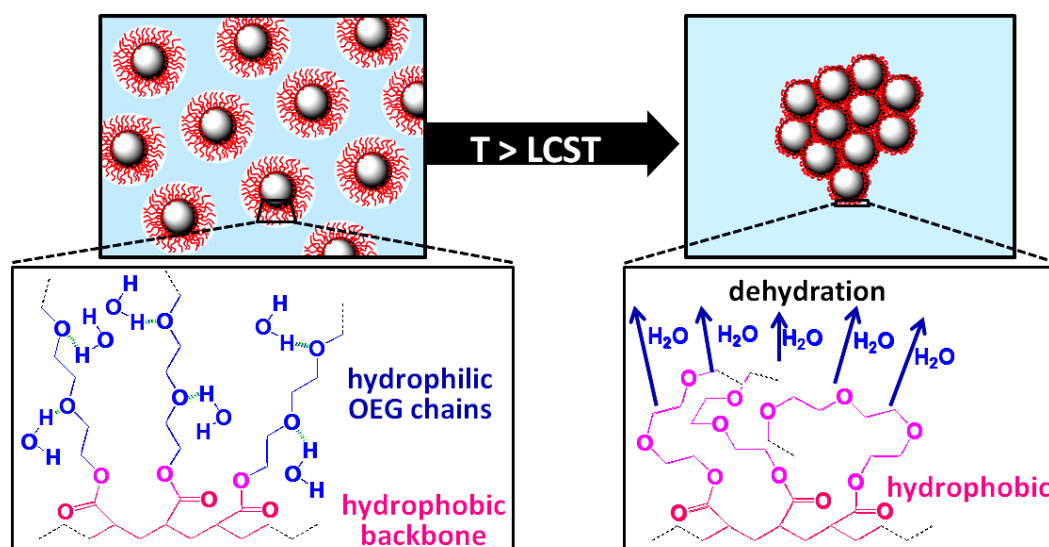


**Fig. S9** Cartoon systemically illustrates the irreversible aggregation of the aqueous dispersion POEGMA-stabilised PPy nanoparticles, which is triggered by dehydration of the grafted POEGMA stabiliser chains when heated above their LCST. Such a thermal transition can be induced via bulk heating or by NIR irradiation. The latter is efficient because the PPy-based particles act as an efficient photothermal transducer.

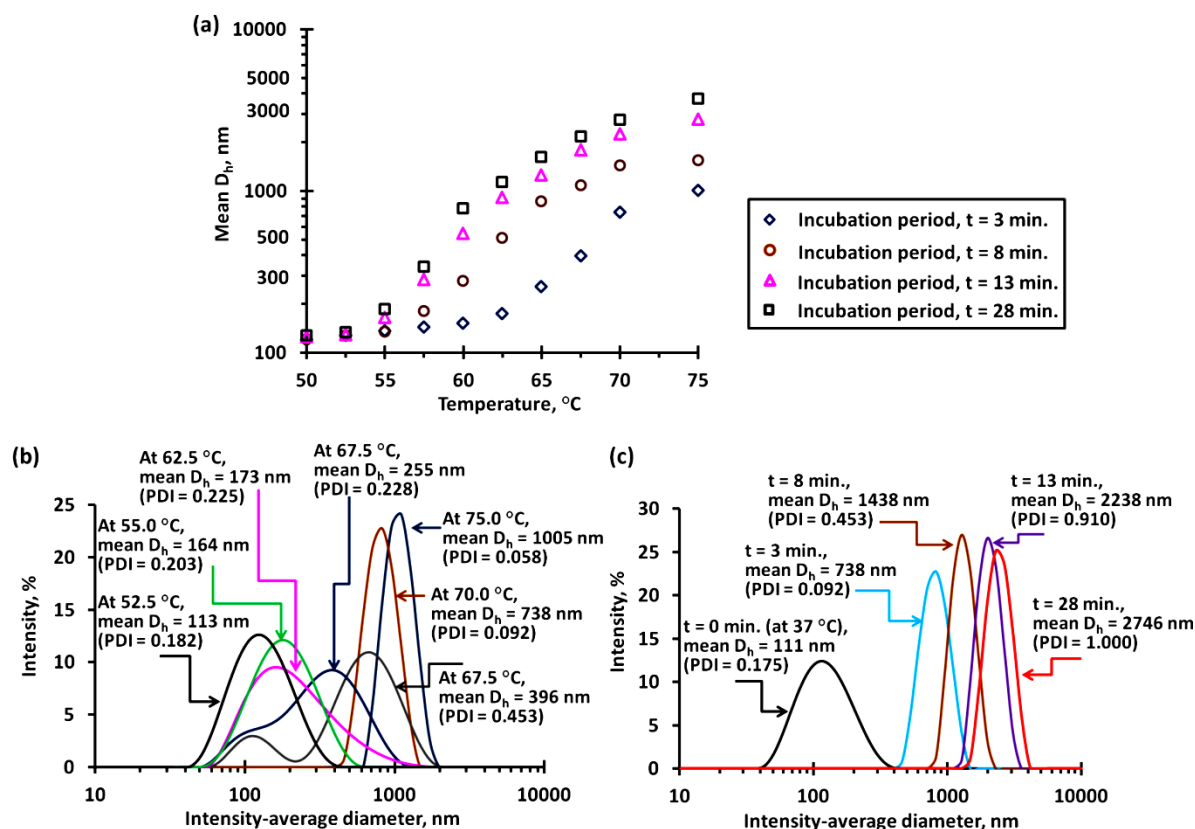


**Fig. S10** (a) Time-dependent DLS studies of POEGMA-stabilised PPy nanoparticles (dispersed in 0.10 M PBS) after incubation at 50 to 75  $^{\circ}\text{C}$  for 3 to 28 min. (b) Intensity-average diameter distribution curves recorded for POEGMA-stabilised PPy nanoparticles after incubation at 52 to 75  $^{\circ}\text{C}$  for 3 minutes. (c) Intensity-average diameter distribution curves for POEGMA-stabilised PPy nanoparticles after incubated at 70  $^{\circ}\text{C}$  for 3 to 28 min. The observed aggregation of the POEGMA-stabilised PPy nanoparticles is triggered by an LCST-type phase transition.

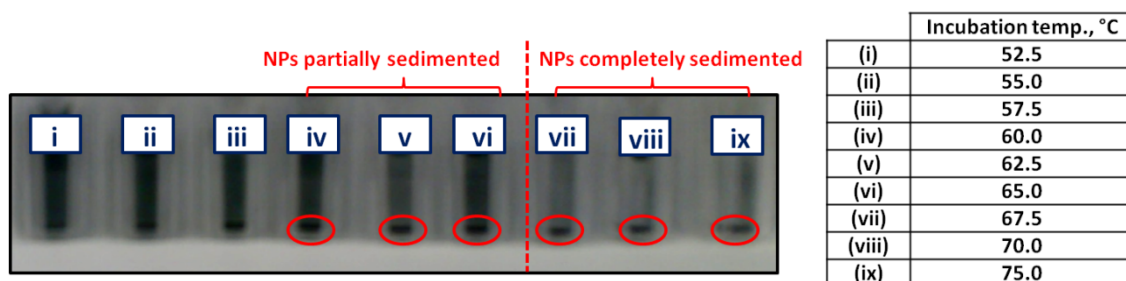


**Fig. S11** Digital photographs recorded for the POEGMA-stabilised PPy nanoparticles (dispersed in 0.10 M PBS) after incubation at 52.5 – 75.0  $^{\circ}\text{C}$  for 3 min. followed by cooling to 20  $^{\circ}\text{C}$  for 24 h. The PPy nanoparticles incubated at above 67.5  $^{\circ}\text{C}$  completely sedimented after cooling to 20  $^{\circ}\text{C}$  for 24 h. The red circles indicate the PPy nanoparticle sediments.

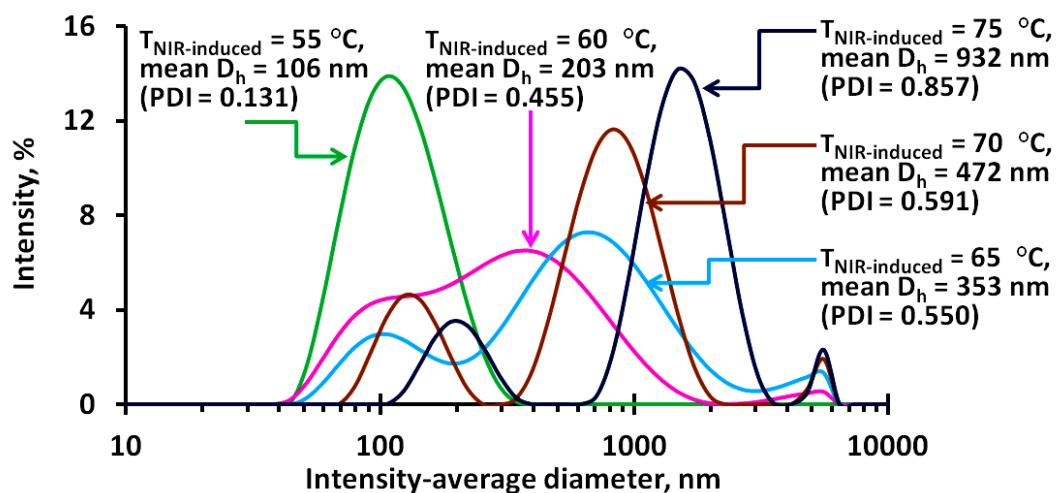


**Fig. S12 (a)** Intensity-average diameter distribution curves recorded for the POEGMA-stabilised PPy nanoparticles (dispersed in 0.10 M PBS) NIR-irradiated (808 nm, 1 Wcm<sup>-2</sup>) to desired temperatures ( $T_{\text{NIR-induced}}$ ) before cooling to 20 °C for 30 min.

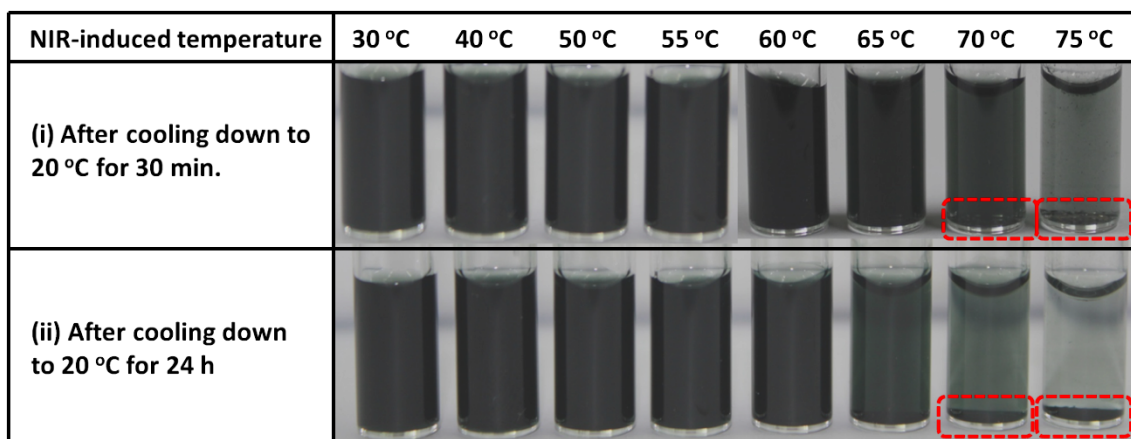


**Fig. S13** Digital photographs obtained after NIR irradiation of POEGMA-stabilised PPy nanoparticles (808 nm, 1.0 W cm<sup>-2</sup>) to attain various temperatures followed by cooling to 20 °C for either 30 min. or 24 h.

## Supporting References

1. K. M. Au, Z. Lu, S. J. Matcher and S. P. Armes, *Biomaterials*, 2013, **34**, 8925-8940.
2. S. P. Armes, J. F. Miller and B. Vincent, *J. Colloid Interface Sci.*, 1987, **118**, 401-416.
3. D. K. Roper, W. Ahn and M. Hoepfner, *J. Phys. Chem. C*, 2007, **111**, 3636-3641.
4. C. M. Hessel, V. P. Pattani, M. Rasch, M. G. Panthani, B. Koo, J. W. Tunnell and B. Korgel, *Nano Lett.*, 2011, **11**, 2560-2566.
5. Q. Tian, F. Jiang, R. Zou, Q. Liu, Z. Chen, M. Zhu, S. Yang, J. Wang, J. Wang and J. Hu, *ACS Nano*, 2011, **5**, 9761-9771.
6. Z. Rawi, J. Mykytiuk and S. P. Armes, *Colloids Surfaces* 1992, **68**, 215-218.
7. S. Kim, W.-K. Oh, Y. S. Jeong, J.-Y. Hong, B.-R. Cho, J.-S. Hahn and J. Jang, *Biomaterials*, 2011, **32**, 2342-2360.
8. Y. S. Jeong, W.-K. Oh, S. Kim and J. Jang, *Biomaterials*, 2011, **32**, 7217-7225.
9. Y. Wang, K. C. L. Black, H. Luehmann, W. Li, Y. Zhang, X. Cai, D. Wan, S.-Y. Liu, M. Li, P. Kim, Z.-Y. Li, L. V. Wang, Y. Liu and Y. Xia, *ACS Nano*, 2013, **7**, 2068-2077.
10. J. L. Bredas and G. B. Street, *Acc. Chem. Res.*, 1985, **18**, 309-315.
11. W. F. Cheong, S. A. Prahel and A. J. Welch, *IEEE J. Quant. Electron.*, 1990, **26**, 2166-2185.
12. J.-F. Lutz, O. Akdemir and A. Hoth, *J. Am. Chem. Soc.*, 2006, **128**, 13046-13047.
13. M. I. Gibson, D. Paripovic and H.-A. Klok, *Adv. Mater.*, 2010, **22**, 4721-4725.
14. L. M. Geever, D. M. Devine, M. J. D. Nugent, J. E. Kennedy, J. G. Lyons, A. Hanley and C. L. Higginbotham, *Eur. Polym. J.*, 2006, **42**, 2540-2548.